Organic & Biomolecular Chemistry

ROYAL SOCIETY OF CHEMISTRY

COMMUNICATION

View Article Online
View Journal

Cite this: DOI: 10.1039/d4ob01037j

Received 22nd June 2024,
Accepted 14th August 2024

DOI: 10.1039/d4ob01037j

rsc.li/obc

A thiol-selective and acid-stable protein modification strategy using an electron-deficient yne reagent†

Zhi-liang Chen, [a,b] Wen Chen, [a] Fenglin Wang, *[a] Jian-Hui Jiang [a] and Wan-Rong Dong *[a]

A protein modification strategy was developed based on a thiol–yne click reaction using an electron-deficient yne reagent. This approach demonstrated exceptional selectivity towards thiols and exhibited rapid kinetics, resulting in conjugates with superior acid stability. The conjugation of IgG with an indole-derived fluorophore was achieved for the imaging of PD-L1 in cancer cells.

Introduction

The chemical conjugation of functional fluorophores or cytotoxins to antibodies holds significant importance in the visualization of biological processes and tumor-targeted therapeutics.[1] As recently reviewed, over 14 antibody–drug conjugates (ADCs) have received approval for cancer treatment, with approximately 100 ADC candidates currently undergoing clinical trials.[2] Developing an excellent conjugation strategy is essential for ensuring the preservation of antibody biological activity, as well as linker stability in a biological environment.

The existing coupling route can be broadly classified into two categories: those involving the incorporation of novel conjugation sites into proteins and those utilizing native amino acid residues on proteins. The first route involves incorporating specific conjugation sites, such as endoglycosidases, unnatural amino acids, and transglutaminase, to enable protein modification through THIOMAB technology,[3] chemoenzymatic strategies,[4] and bioorthogonal reactions.[5] The second route involves utilizing chemical reactions that rely on endogenous amino acid residues like cysteine (Cys), lysine, and tyrosine for the covalent attachment of cytotoxins.[6] Over the past two decades, significant advancements have been made in both routes. The former exhibits certain advantages over the latter in terms of site-specific coupling and the high heterogeneity of protein conjugations. However, the first strategy also presents evident drawbacks, including procedural complexity, time consumption, and the requirement for advanced technical expertise. The utilization of proteinogenic amino acids as a preferred conjugation site remains highly favored in various situations, particularly within the context of clinical trials.[1a,2]

Among proteinogenic amino acids, the Cys residue exhibits high nucleophilicity, which confers a distinct advantage in facilitating rapid protein conjugation. Moreover, the limited abundance of surface-exposed Cys ensures a precise and thiol-selective conjugation site with minimal perturbation to protein activity.[7] Considering the aforementioned advantages, numerous Cys-based reactions have been developed for antibody modification in both commercial applications and scientific research, including maleimide and its derivatives,[8] photo-catalytically generated sulfoxonium ion reagents,[9] carbonylacrylic reagents,[10] ethynyl-triazolyl-phosphinate reagents,[11] and chlorofluoroacetamide reagents,[12] among others.[13] The above-mentioned electrophile reagents demonstrate advancements in selectivity towards Cys and the stability of conjugates under physiological conditions. However, the generation of these electrophile reagents involves complex and intricate multi-step processes, requiring a high level of technical expertise, which can potentially complicate bioconjugation procedures. The fields of bioimaging and tumor-targeted therapeutics are still eagerly anticipating a protein conjugation method that satisfies the criteria of procedural simplicity, rapid reaction kinetics, and high stability in mildly acidic environments.

Here, we have developed a protein conjugation strategy based on a thiol–yne click reaction, utilizing an electron-deficient yne reagent (Fig. 1a). The electrophilic moiety of the electron-deficient yne reagent was designed by incorporating an electron-withdrawing ester group into the ethynyl group.[14] We have demonstrated the high selectivity of this prepared yne reagent towards Cys, as well as its rapid kinetics under mild reaction conditions. Furthermore, we observed that the resulting adducts remain highly stable even under acidic conditions

[a]State Key Laboratory of Chemo/Biosensing & Chemometrics, College of Chemistry & Chemical Engineering, Hunan University, Changsha 410082, China.
E-mail: wanrongdong@hnu.edu.cn, fengliw@hnu.edu.cn
[b]School of Pharmacy, Shaoyang University, Shaoyang, 422000, P. R China

†Electronic supplementary information (ESI) available: Regents, synthesis methods and detailed material characterization. See DOI: https://doi.org/10.1039/d4ob01037j

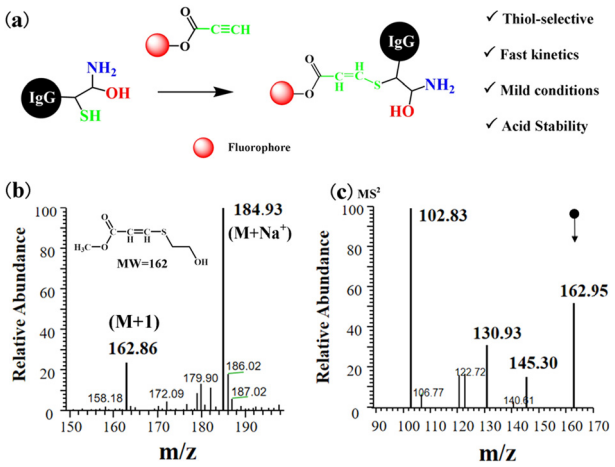

Fig. 1 (a) Scheme of thiol-selective bioconjugation using an electron-deficient yne reagent. (b) MS spectrum of the methyl propiolate-β-mercaptoethanol adduct. (c) MS–MS spectrum of the adduct peak at *m*/*z* 162.95.

and in the presence of sulfhydryl-containing compounds. Subsequently, an yne-containing fluorophore was synthesized and utilized for the conjugation of immunoglobulin G (IgG), which was further employed for imaging programmed death ligand 1 (PD-L1), an immune checkpoint inhibitor, in MCF-7 and HepG-2 cells. Our thiol–yne click reaction offers several advantages compared to previous strategies. First, the synthesis of the ester-functionalized yne reagent is simple and convenient, which can facilitate the derivation of fluorophores or drugs with hydroxyl groups for subsequent bioconjugation and biolabeling purposes. Second, the thiol–yne reaction exhibits remarkable selectivity towards Cys residues, allowing for thiol-specific protein conjugation with minimal disruption to their activity. Third, the resulting thiol–yne conjugates exhibit exceptional stability under mild acidic conditions in the presence of the thiol group. We believe that the thiol–yne click reaction offers a valuable strategy for conjugating and labeling antibodies.

Results and discussion

To explore the feasibility of the thiol–yne click reaction, we initially selected methyl propiolate and β-mercaptoethanol as models to illustrate the concept. A new absorption peak at 286 nm was observed upon incubation of mercaptoethanol with methyl propiolate in an aqueous solution at 25 °C for 2 h (Fig. S1, ESI†). No absorption peaks were observed at 286 nm for either methyl propiolate or β-mercaptoethanol alone under the same experimental conditions. The obtained results suggest the formation of new substances with an extended conjugation system through the incubation of mercaptoethanol with methyl propiolate. The mass spectrum (MS) showed two peaks at *m*/*z* 184.93 and 162.95, respectively, corresponding to $[M + H]^+$ and $[M + Na]^+$ of the thiol–yne adduct (Fig. 1b). We further analyzed the peak at *m*/*z* 162.86 using tandem mass spectrometry (MS-MS). As displayed in Fig. 1c, the peak at *m*/*z* 145.3 indicated the loss of hydroxyl groups from the adduct, suggesting that our thiol–yne click-reaction involved the selective formation of a sulfur–carbon bond in the presence of a hydroxyl group. The potential fragmentation pathways for the corresponding adduct peak at *m*/*z* 162.95 were proposed and presented in Fig. S2 (ESI†). The thiol–yne adducts were further purified by silica gel chromatography and confirmed by ^{1}H NMR spectroscopy (Fig. S3 and S4, ESI†). These results provide direct evidence for the formation of thiol–yne adducts, thereby demonstrating the successful coupling between methyl propiolate and β-mercaptoethanol. In contrast, no new absorption peak was observed after incubating propargylamine with β-mercaptoethanol under identical conditions (Fig. S5, ESI†). This result indicated that the electron-deficient yne group is advantageous for the thiol–yne reaction, which is consistent with previous reports.[15] Moreover, a peak at *m*/*z* 162.03 was observed in the presence of methyl propiolate and 2-aminoethanethiol, suggesting the formation of a thiol–yne adduct (Fig. S6, ESI†). The MS–MS spectrum displayed a peak at *m*/*z* 144.3, which could be attributed to the loss of a primary amine from the adduct (Fig. S7 and S8, ESI†). Further reaction of methyl propargynate with a tetrapeptide (Cys–Ser–Tyr–Ala) confirmed the high selectivity of the thiol–yne reaction in the presence of both primary amine and hydroxyl groups (Fig. S9–S11, ESI†). These findings collectively demonstrate that the thiol–yne reaction could be selectively achieved in the presence of primary amine and hydroxyl groups.[16] The selective thiol–yne reaction described here offers significant advantages for homogeneous protein conjugation. Furthermore, its capacity to react with Cys and glutathione (GSH) was thoroughly investigated. Notably, distinct absorption peaks emerged upon incubating methyl propiolate with Cys or GSH (Fig. S12 and S13, ESI†), providing compelling evidence of the successful coupling between methyl propiolate and Cys or GSH.

We further investigated the reaction kinetics between methyl propiolate and β-mercaptoethanol by monitoring the absorption peak of the resulting adducts at 286 nm. As depicted in Fig. 2a, the absorbance at 286 nm gradually increased over time when methyl propiolate and β-mercaptoethanol were reacted at pH values ranging from

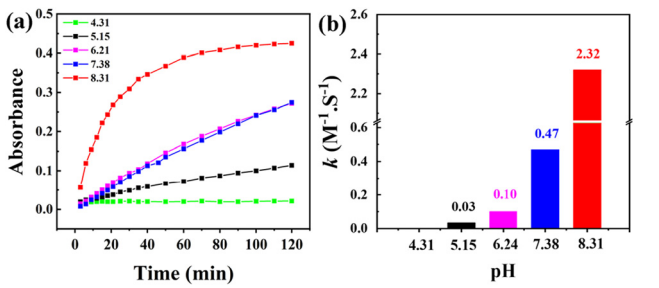

Fig. 2 (a) Time course of absorbance variations for monitoring the reaction of methyl propiolate with β-mercaptoethanol at different pH values. (b) Reaction rate constants at different pH values ranging from 4.31 to 8.31.

5.15 to 8.31 (Fig. 2b and S14, ESI†). Moreover, the largest increase in absorbance was observed for reactions conducted at pH 8.31, while there was negligible change in absorbance for those carried out at pH 4.31. Specifically, the reaction rate constants increased from 0.03 M^{-1} S^{-1} to 2.32 M^{-1} S^{-1} as the pH changed from 5.15 to 8.31 at 25 °C. These results indicated that an alkaline environment is advantageous for enhancing the reaction rates, which aligns with previous findings.[17] We further assessed the reaction rates of the thiol–yne reaction at different temperatures and observed a predictable increase in reaction kinetics with increasing temperature (Fig. S15, ESI†). These findings underscored the relatively rapid reaction kinetics associated with thiol conjugation, which could be attributed to the incorporation of an electron-withdrawing ester bond into the yne motif. The stability of conjugates under mild acidic conditions and in the presence of thiols is crucial for their effectiveness in tumor-related applications. Subsequently, we investigated the stability of the methyl propiolate-β-mercaptoethanol adducts under different pH condition. Furthermore, we compared its stability to that of maleimide-β-mercaptoethanol adducts, which is a commonly employed strategy for antibody conjugation. The thiol–yne and maleimide–thiol adducts were incubated with varying concentrations of Cys within the pH range of 4.31–8.31, and absorption spectra were obtained at different time points for a duration of up to 7 days. The thiol–yne adduct demonstrated excellent stability in the presence of 350 μM Cys, maintaining its integrity as the pH varied from 4.31 to 7.38 over a period of 7 days (Fig. 3a, b and S16, ESI†). As displayed in Fig. 3c, over 70% of thiol–yne adducts exhibited stability when incubated with Cys (1 mM) at pH levels ranging from 4.31 to 6.24 for a duration of 7 days, while approximately 60% of the adducts retained their stability after incubation with Cys (1 mM) at pH levels between 7.38 and 8.31. In contrast, the stability of the maleimide-β-mercaptoethanol adduct decreased as both the concentrations of Cys increased and the pH decreased (Fig. 3d–f and S17, ESI†). About half the adducts lost their stability within one week in the presence of Cys (1 mM), consistent with previous reports indicating that maleimide-β-mercaptoethanol adducts are susceptible to thiol exchange.[18] We further explored the stability of methyl propiolate-β-mercaptoethanol adducts in the presence of Cys (1.5 mM). The thiol–yne adducts remained stable under acidic conditions ranging from pH 4.31 to 6.24 (Fig. S18a, ESI†), but exhibited a more than 50% decrease in stability between pH 7.38 and 8.31, likely attributed to ester hydrolysis under alkaline conditions. This instability of ester groups may prevent their application under alkaline conditions. Direct evidence for ester hydrolysis was obtained through MS and MS–MS spectrometry analysis of the degraded product (Fig. S19 and S20, ESI†). Meanwhile, the methyl propiolate-β-mercaptoethanol adducts also exhibited good acid stability in the presence of GSH (Fig. S18b†). These results demonstrated the exceptional acid stability of the thiol–yne conjugates in the presence of exogenous thiols, thereby supporting their advantageous application as protein conjugates under mild acidic conditions.

Reinvigorated by the above-mentioned advantages of rapid reaction kinetics and robust linker stability, we proceeded to explore the potential for antibody conjugation. Initially, we designed a fluorophore (Scheme S2, ESI†), IB-Y, through the reaction of indole with benzenamine and subsequent deri-

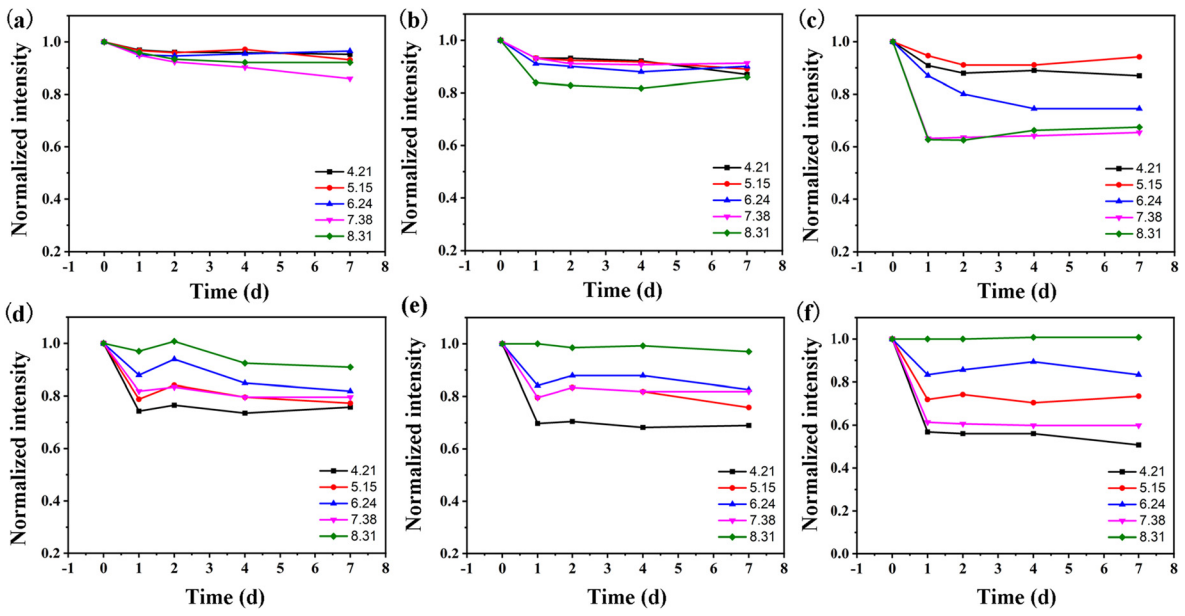

Fig. 3 (a) Aqueous stability of adducts in the presence of various concentrations of Cys under different pH conditions. (a–c) Methyl propiolate-β-mercaptoethanol adduct incubated with 0 (a), 350 μM (b) and 1 mM (c) Cys at pH 4.21–8.31 for 7 days at room temperature. (d–f) Maleimide-β-mercaptoethanol adduct incubated with 0 (d), 350 μM (e) and 1 mM (f) Cys at pH 4.21–8.31 for 7 days at room temperature.

vation with an electron-deficient yne group. The successful synthesis and characterization of IB-Y were confirmed (Fig. S21–S24, ESI†). Notably, IB-Y displayed an absorption peak at approximately 540 nm and exhibited a fluorescence emission maximum at 615 nm (Fig. S21, ESI†). To facilitate the conjugation of goat anti-mouse IgG, the interchain disulfide bonds were reduced using dithiothreitol (DTT) and subsequently incubated with IB-Y (Fig. 4a).[10,15a,19] We utilized the sodium dodecyl sulfate-polyacrylamide gel electrophoresis (SDS-PAGE) technique to examine the conjugated products, denoted as IgG-IB. As depicted in Fig. 4b, SDS-PAGE analysis revealed four distinct bands that exhibited high fluorescence intensity upon excitation at 530 nm. These bands could be attributed to the complete IgG, half IgG, heavy chains, and light chains, respectively.[15a,19] Notably, the fluorescent bands observed for IgG-IB were narrow and devoid of any noticeable smearing, indicating the successful attainment of homogeneous conjugation.

We further investigated the imaging capability of IgG-IB for visualizing PD-L1, a prototypical immune checkpoint inhibitor that is overexpressed on cancer cells. Initially, we selected human hepatocellular carcinoma (HepG2) cells with elevated levels of PD-L1 as a demonstration model. Following fixation, HepG2 cells were subjected to treatment with primary antibodies against mouse PD-L1 (Fig. 4c), followed by staining with IgG-IB conjugates. Immunofluorescence imaging revealed intense red fluorescence originating from IgG-IB (Fig. 4d). The fluorescence was observed both on the inner cell membrane and within the cytosol, probably attributed to the penetration of the PD-L1 primary antibody, which is consistent with previous findings.[20] A negligible red fluorescence signal was observed in control HepG2 cells that were not treated with the PD-L1 primary antibody (Fig. 4e and f). Similarly, consistent immunofluorescence imaging results were obtained for MCF-7 breast cancer cell line cells (Fig. S25, ESI†). The obtained results suggest that the targeted recognition of IgG remained unaltered following the thiol–yne click reaction with IB-Y, thereby demonstrating the preservation of antibody bioactivity.

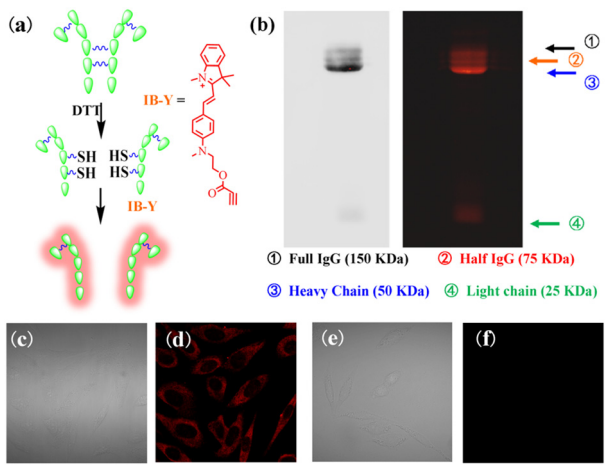

Fig. 4 (a) Schematic of the conjugation of IgG with IB-Y. (b) SDS-PAGE analysis of IgG-IB. Left: Coomassie blue mode and right: fluorescence mode. Immunofluorescence images of fixed HepG2 cells treated with (c and d) or without (e and f) the PD-L1 primary antibody and stained with IgG-IB conjugates. Bright field (c and e) and fluorescence images (d and f).

Conclusions

In summary, we presented an excellent protein modification approach using an electron-deficient yne reagent. This modification strategy exhibits rapid reaction kinetics and demonstrates remarkable selectivity towards thiols, resulting in protein conjugates that possess superior acid stability even in the presence of exogenous thiols. Moreover, a fluorescent IB-Y probe was synthesized to enable the visualization of PD-L1 in MCF-7 and HepG-2 cells, thereby highlighting the versatility of the thiol–yne click reaction as a powerful tool for antibody conjugation and biolabeling. In future studies, the applications of thiol–yne click reactions for antibody conjugation will be explored.

Authorship contribution

Zhi-Liang Chen conducted the experiments and prepared the original draft of the manuscript. Wen Chen performed the formal analysis and curated the data. Fenglin Wang and Wan-Rong Dong contributed to reviewing and editing the manuscript. Jian-Hui Jiang participated in data curation.

Data availability

The data supporting this article are available in both the main text and its ESI.†

Conflicts of interest

There are no conflicts to declare.

Acknowledgements

This work was supported by the National Key Research Program (2019YFA0905800 and 2018YFA0902301), NSFC Programs (21991084, 21904034 and 22090053) and the Hunan Provincial Science Fund for Distinguished Young Scholars (2022JJ10004).

References

1 (*a*) T. Journeaux and G. J. L. Bernardes, *Nat. Chem.*, 2024, **16**, 854–870; (*b*) A. V. Ramsey, A. J. Bischoff and M. B. Francis, *J. Am. Chem. Soc.*, 2021, **143**, 7342–7350; (*c*) R. C. Griffiths, F. R. Smith, J. E. Long, D. Scott,

H. E. L. Williams, N. J. Oldham, R. Layfield and N. J. Mitchell, *Angew. Chem., Int. Ed.*, 2022, **61**, e202110223.
2 Y. Zeng, W. Shi, Q. Dong, W. Li, J. Zhang, X. Ren, C. Tang, B. Liu, Y. Song, Y. Wu, X. Diao, H. Zhou, H. Huang, F. Tang and W. Huang, *Angew. Chem., Int. Ed.*, 2022, **61**, e202204132.
3 J. R. Junutula, H. Raab, S. Clark, S. Bhakta, D. D. Leipold, S. Weir, Y. Chen, M. Simpson, S. P. Tsai, M. S. Dennis, Y. Lu, Y. G. Meng, C. Ng, J. Yang, C. C. Lee, E. Duenas, J. Gorrell, V. Katta, A. Kim, K. McDorman, K. Flagella, R. Venook, S. Ross, S. D. Spencer, W. L. Wong, H. B. Lowman, R. Vandlen, M. X. Sliwkowski, R. H. Scheller, P. Polakis and W. Mallet, *Nat. Biotechnol.*, 2008, **26**, 925–932.
4 T. J. Harmand, D. Bousbaine, A. Chan, X. Zhang, D. R. Liu, J. P. Tam and H. L. Ploegh, *Bioconjugate Chem.*, 2018, **29**, 3245–3249.
5 B. Oller-Salvia, G. Kym and J. W. Chin, *Angew. Chem., Int. Ed.*, 2018, **57**, 2831–2834.
6 (*a*) O. Konievab and A. Wagner, *Chem. Soc. Rev.*, 2015, **44**, 5495–5551; (*b*) M. S. Kang, T. W. S. Kong, J. Y. X. Khoo and T.-P. Loh, *Chem. Sci.*, 2021, **12**, 13613–13647; (*c*) N. C. Reddy, M. Kumar, R. Molla and V. Rai, *Org. Biomol. Chem.*, 2020, **18**, 4669–4691.
7 (*a*) R. N. Reddi, A. Rogel, E. Resnick, R. Gabizon, P. K. Prasad, N. Gurwicz, H. Barr, Z. Shulman and N. London, *J. Am. Chem. Soc.*, 2021, **143**, 20095–20108; (*b*) C. Sornay, V. Vaur, A. Wagner and G. Chaubet, *R. Soc. Open Sci.*, 2022, **9**, 211563; (*c*) S. Sato, K. Nakane and H. Nakamura, *Org. Biomol. Chem.*, 2020, **18**, 3664–3668.
8 D. Kalia, P. V. Malekar and M. Parthasarathy, *Angew. Chem., Int. Ed.*, 2016, **55**, 1432–1435.
9 C. Wan, Z. Hou, D. Yang, Z. Zhou, H. Xu, Y. Wang, C. Dai, M. Liang, J. Meng, J. Chen, F. Yin, R. Wang and Z. Li, *Chem. Sci.*, 2023, **14**, 604–612.
10 B. Bernardim, M. J. Matos, X. Ferhati, I. Compañti, A. Guerreiro, P. Akkapeddi, A. C. B. Burtoloso, G. Jiménez-Osés, F. Corzana and G. J. L. Bernardes, *Nat. Protoc.*, 2019, **14**, 86–99.
11 M.-A. Kasper, A. Stengl, P. Ochtrop, M. Gerlach, T. Stoschek, D. Schumacher, J. Helma, M. Penkert, E. Krause, H. Leonhardt and C. P. R. Hackenberger, *Angew. Chem., Int. Ed.*, 2019, **58**, 11631–11636.
12 N. Shindo, H. Fuchida, M. Sato, K. Watari, T. Shibata, K. Kuwata, C. Miura, K. Okamoto, Y. Hatsuyama, K. Tokunaga, S. Sakamoto, S. Morimoto, Y. Abe, M. Shiroishi, J. M. M. Caaveiro, T. Ueda, T. Tamura, N. Matsunaga, T. Nakao, S. Koyanagi, S. Ohdo, Y. Yamaguchi, I. Hamachi, M. Ono and A. Ojida, *Nat. Chem. Biol.*, 2019, **15**, 250–258.
13 P. Chauhan, V. Ragendu, M. Kumar, R. Molla, S. D. Mishra, S. Basa and V. Rai, *Chem. Soc. Rev.*, 2024, **53**, 380–449.
14 T. C. Owen, *Bioorg. Chem.*, 2008, **36**, 156–160.
15 (*a*) H.-Y. Shiu, T.-C. Chan, C.-M. Ho, Y. Liu, M.-K. Wong and C.-M. Che, *Chem. – Eur. J.*, 2009, **15**, 3839–3850; (*b*) M.-A. Kasper, M. Glanz, A. Stengl, M. Penkert, S. Klenk, T. Sauer, D. Schumacher, J. Helma, E. Krause, M. C. Cardoso, H. Leonhardt and C. P. R. Hackenberger, *Angew. Chem., Int. Ed.*, 2019, **58**, 11625–11630.
16 (*a*) B. Song, D. Lu, A. Qin and B.-Z. Tang, *J. Am. Chem. Soc.*, 2022, **144**, 1672–1680; (*b*) Y. Zhang, J. Shen, R. Hu, X. Shi, X. Hu, B. He, A. Qin and B. Z. Tang, *Chem. Sci.*, 2020, **11**, 3931–3935.
17 E. Petit, L. Bosch, A. M. Costa and J. Vilarrasa, *J. Org. Chem.*, 2019, **84**, 11170–11176.
18 (*a*) C. E. Stieger, L. Franz, F. Kçrlin and C. P. R. Hackenberger, *Angew. Chem., Int. Ed.*, 2021, **60**, 15359–15364; (*b*) J. F. Ponte, X. Sun, N. C. Yoder, N. Fishkin, R. Laleau, J. Coccia, L. Lanieri, M. Bogalhas, L. Wang, S. Wilhelm, W. Widdison, J. Pinkas, T. A. Keating, R. Chari, H. K. Erickson and J. M. Lambert, *Bioconjugate Chem.*, 2016, **27**, 1588–1598.
19 P. A. Szijj, C. Bahou and V. Chudasama, *Drug Discovery Today*, 2018, **30**, 27–34.
20 H. Polioudaki, A. Chantziou, K. Kalyvianaki, P. Malamos, G. Notas, D. Mavroudis, M. Kampa, E. Castanas and P. A. Theodoropoulos, *Cell. Oncol.*, 2019, **42**, 237–241.